

Selective, Stable Production of Ethylene Using a Pulsed Cu-Based Electrode

Jian Zhang, Zhipeng Liu, Hongshan Guo, Haoran Lin, Hao Wang, Xiao Liang, Hanlin Hu, Qibin Xia, Xiaoxin Zou,* and Xiaoxi Huang*



Cite This: <https://doi.org/10.1021/acsami.2c01230>



Read Online

ACCESS |



Metrics & More



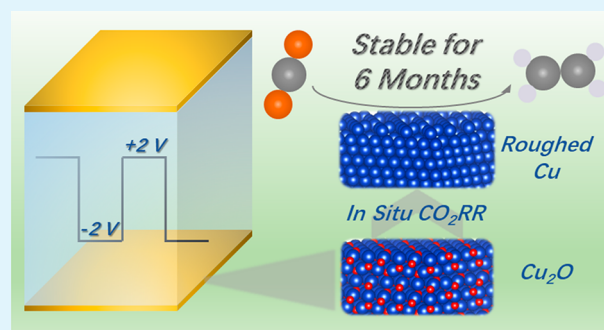
Article Recommendations



Supporting Information

ABSTRACT: Ethylene (C_2H_4) is an important product in carbon dioxide electroreduction (CO_2RR) because of the essential role it plays in chemical industry. While several strategies have been proposed to tune the selectivity of Cu-based catalysts in order to achieve high C_2H_4 faradaic efficiency, maintaining high selectivity toward C_2H_4 in CO_2RR remains an unresolved problem hampering the deployment of CO_2 conversion technology due to the lack of stable electrocatalysts. Here, we develop a facile method to deposit a layer of Cu_2O on Cu foil by an electrochemical pulsed potential treatment. This method is capable to easily scale up and synthesize multiple electrodes in one step. After the synthesis, the pulsed copper foil, denoted as P-Cu, exhibits good C_2H_4 faradaic efficiency of $\sim 50\%$ in CO_2RR at a potential around -1.0 V vs. RHE. The C_2H_4 selectivity is also found to be quantitatively correlated with the roughness factor (RF) of Cu-based catalysts. More importantly, for the first time, we demonstrate that the P-Cu electrode is quite durable in CO_2RR to produce C_2H_4 for more than 6 months.

KEYWORDS: CO_2 electroreduction, copper catalyst, hydrocarbons, pulsed synthesis, stability, ethylene



1. INTRODUCTION

Environmental awareness regarding the carbon cycle has been rapidly growing because of the serious climate crisis caused by the increasing level of carbon dioxide in the atmosphere. The effective conversion of carbon dioxide to value-added chemicals powered by renewable electricity is promising, since the electricity derived from intermittent clean energy sources has become more prevalent with lower cost.¹ However, due to the lack of high-performance electrocatalysts for CO_2RR , the time is not ripe for practical application of CO_2RR . Among various metal catalysts, copper-based materials have received the most attention because of their ability to convert CO_2 into more valuable hydrocarbons and oxygenates.^{2,3} But controlling the product selectivity in CO_2RR still faces serious difficulties; for example, a total of 16 different products were identified on a metallic copper electrode during CO_2RR .⁴ In particular, achieving high C_2H_4 faradaic efficiency is challenging because of the large energy barriers for C–C bond formation and the existence of multiple competing reaction pathways.^{5–7}

There are several strategies that can tune the surface electronic/geometric structures of Cu-based catalysts to promote the faradaic efficiency of multicarbon products, including but not limited to molecular functionalization,^{8,9} surface roughening,¹⁰ nanostructuring,^{11,12} and facet engineering.^{13–16} Noteworthy ones are various oxide-derived rough Cu

catalysts, as they can not only reduce the overpotentials for CO_2RR but also increase the production rate of multicarbon products.^{17–19} However, copper-based electrocatalysts are vulnerable to reconstruction, losing the rough surface during CO_2RR and consequently leading to the undesirable change of catalytic activity and/or selectivity.^{20–23} Although the long-term generation of CO has been achieved by silver catalysts for thousands of hours,^{24,25} the studies of CO_2RR to produce C_2H_4 by Cu catalysts are generally limited to a few to tens of hours; only a very few reports demonstrate the ability to operate for hundreds of hours.²⁶ Therefore, exploring appropriate methods to synthesize higher-performance Cu-based catalysts for CO_2 -to- C_2H_4 conversion over a longer time span (e.g., thousands of hours) is essential and still remains a major challenge. Apart from the stability of the catalyst itself, other problems, such as the flooding issue and the formation of carbonate salt, can lead to cathode malfunction when operating at high current density on the gas diffusion electrode (GDE). The declined performance in a flow cell utilizing a GDE is very

Received: January 20, 2022

Accepted: April 13, 2022



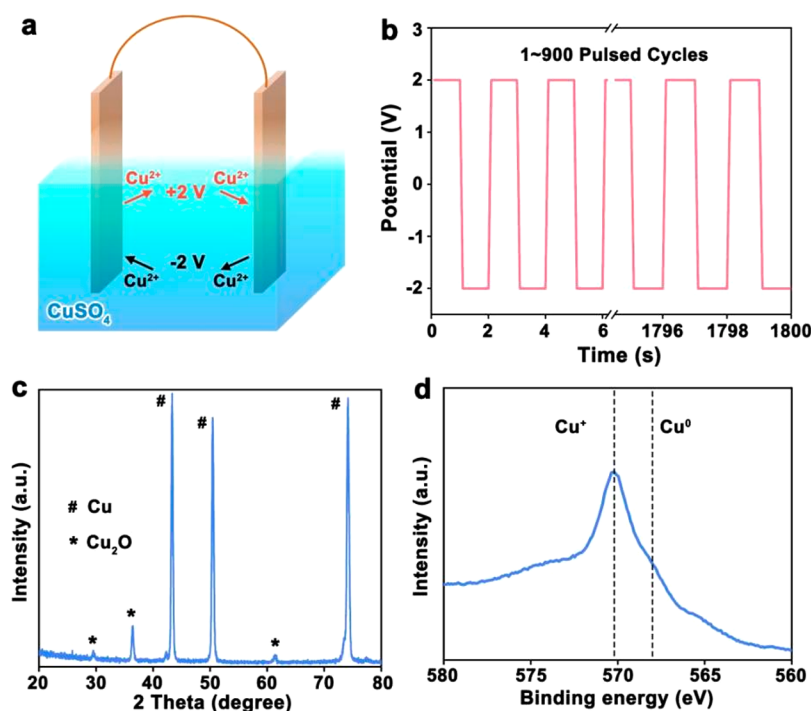


Figure 1. (a) Schematic illustration of the setup for pulsed synthesis. (b) The potential values applied between two electrodes for pulsed synthesis. (c) GIXRD pattern and (d) Cu LMM Auger spectrum of P-Cu.

complicated and could be associated with multiple factors, including but not limited to the loss of an active catalytic surface, the change of the hydrophobic interface, and the accumulation of carbonate salts.²⁷ Conversely, CO₂RR in an H-cell albeit can only operate at a small current density, has neither a flooding issue nor a salt deposition problem, making it a suitable tool to study the long-term stability of a catalyst itself.

To this end, we develop a scalable pulsed potential method to synthesize a highly active Cu-based electrocatalyst and investigate the long-term stability of CO₂-to-C₂H₄ conversion in an H-cell. The electrochemical CO₂RR studies demonstrate that the pulsed copper foil, denoted as P-Cu, gives a high faradaic efficiency (FE, ~50%) toward C₂H₄. The high C₂H₄ selectivity is ascribed to the rough surface with an increased electrochemical surface area (ECSA). Besides favorable selectivity toward C₂H₄, the P-Cu electrode can electrocatalyze CO₂RR with stable C₂H₄ production for ~4500 h, which is over 6 months. This is the first report that a Cu-based CO₂RR electrocatalyst maintains good C₂H₄ selectivity in the time span of thousands of hours.

2. RESULTS AND DISCUSSION

2.1. Synthesis and Characterization of Electrocatalysts. The setup for pulsed synthesis of the copper catalyst is shown in Figure 1a. Multiple cycles of pulsed potentials at ± 2 V were applied between two Cu foils in 0.1 M CuSO₄ electrolyte (Figure 1b). The corresponding current–time curves are displayed in Figure S1 in the Supporting Information (SI). During the pulsed potential treatment, the anodic currents and cathodic currents are observed repeatedly, implying that oxidation/reduction reactions happen on the surfaces of two Cu foils alternatively. One of the pulsed Cu foils from the two-electrode system is characterized first. The grazing incident X-ray diffraction (GIXRD) pattern of the P-

Cu material (i.e., the Cu foil by 900 pulsed cycles) is displayed in Figure 1c. Besides the primary peaks associated with the metallic copper substrate, there are several new features at 2θ of 36.4, 29.6, and 61.4°, corresponding to the (111), (110), and (220) planes of Cu₂O. The high-resolution X-ray photoelectron spectrum (XPS) of the Cu LMM of the P-Cu material was collected, and the result is shown in Figure 1d. The signals at 568.2 and 570.3 eV are ascribed to Cu⁰ and Cu¹⁺ species, respectively.^{28,29} After pulsed synthesis, P-Cu primarily displays a peak at 570.3 eV, indicating the oxidation number of surface Cu is +1. In conclusion, the above results confirm that Cu₂O is deposited on the Cu surface after pulsed synthesis.

SEM was used to investigate the morphology of Cu foils at different synthetic stages. The polished Cu foil is very flat with a negligible amount of defective structures (Figure 2a). After 10 cycles of pulsed synthesis, the smooth surface became roughened; meanwhile, there are many nanoparticles with various shapes observed on the surface (Figure 2b). Some of them have octahedral shapes exposing eight triangle faces, which are ascribed to the Cu₂O (111) facet. Some of them are truncated octahedral particles exposing Cu₂O (100) facets in addition to Cu₂O (111) facets. Many particles are embedded in the underneath substrate partially. Similar polyhedral Cu₂O nanoparticles exposing specific crystal facets were reported previously.¹⁶ In terms of P-Cu after 900 cycles of synthesis, the well-defined nanoparticles are absent (Figure 2c), but the surface is still rough, implying that the nanoparticles may have merged together to form a continuous film. It is likely that the merging process may generate defective structures more easily when reduced in the process of CO₂RR, such as grain boundaries, which have been proved as active sites for the conversion of CO₂ or CO to C₂+ products.^{30–32} Based on the above observation, we propose a growth mechanism for Cu₂O film. During the initial pulsed cycling, isolated Cu₂O particles

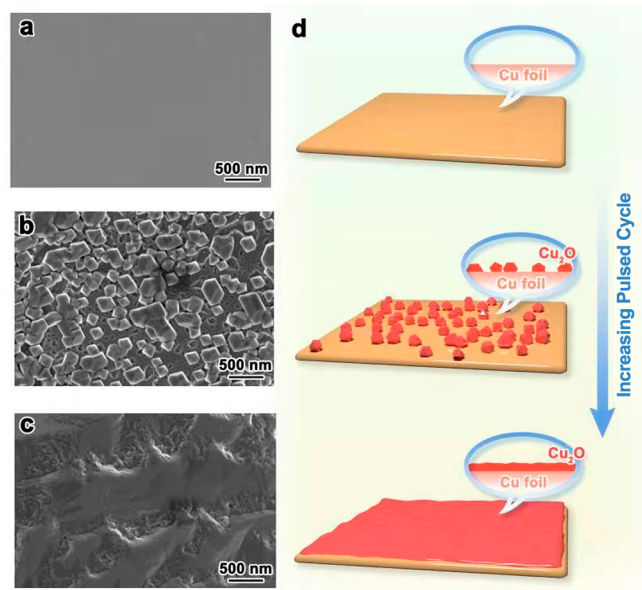


Figure 2. SEM images of (a) polished Cu and P-Cu synthesized with (b) 10 cycles or (c) 900 cycles. (d) Schematic illustration of surface structure changes during pulsed synthesis.

start to nucleate and grow into polyhedral particles; after a prolonging pulsed cycling time, the randomly oriented particles become more aggregated and eventually form a continuous, rough Cu₂O film (Figure 2d). This kind of catalytic film is essential for durable and selective C₂H₄ production in CO₂RR, whereas the film composed of isolated polyhedral Cu₂O nanoparticles could not achieve such a performance (see the results and discussion after).

It should be noted that during pulsed synthesis the observed anodic currents roughly equal with cathodic currents at the absolute value of ~40 mA (Figure S1, SI). This is likely because the initial two Cu foils are identical with each other and the applied pulsed voltage values are symmetric. Consequently, it is expected that the structural characteristics of both Cu foils would be similar after the pulsed synthesis. This is confirmed by GIXRD (Figure S2, SI) and SEM (Figure S3, SI) results of the other electrode. In addition, by connecting more Cu foils in parallel, this method is able to produce multiple electrocatalysts simultaneously (Figure 3a), and we showed an example to synthesize 10 P-Cu electrodes at the same time (Figure S4, SI). Furthermore, two large Cu foils with 10 × 10 cm dimensions were used as starting materials for pulsed synthesis, showing the ability to scale the areas of electrode from 1 to 100 cm² (Figure 3b).

Oxide-derived Cu-based CO₂RR electrocatalysts have been synthesized by many approaches, for example, thermal annealing,^{18,19,30} hydrothermal treatment,³³ electrochemical method,^{13,28,34–37} chemical oxidation,^{38,39} plasma treatment,⁴⁰ or a combination of several synthetic strategies.^{41,42} Compared with these methods, our strategy at least features the following advantages: (i) two of the same Cu-based electrodes can be synthesized at the same time in a standard two-electrode system; (ii) the number of electrodes could be increased by using more parallel Cu foils; (iii) the size of electrode could be enlarged to meet the requirement of practical applications.

2.2. CO₂RR Catalytic Activity Evaluation. Next, the CO₂RR performance was evaluated in a gas-tight H-cell in 0.1 M KHCO₃ by using the above P-Cu catalysts directly without further treatment. P-Cu catalysts synthesized with 10 cycles and 900 cycles are denoted as P-Cu-1 and P-Cu-2, respectively. The constant potential electrolysis was conducted at several potential values. As displayed in Figure 4a, the total geometric current densities are higher on the P-Cu catalysts after pulsed synthesis compared with polished Cu foil, in part because their surfaces are rougher as shown in SEM images. Polished Cu foil favors CH₄ over C₂H₄ in CO₂RR (Figure 4b). At −1.28 V vs RHE, the FE of CH₄ is the highest at 57.9%, while the number for C₂H₄ is below 5% for the polished Cu foil. In contrast, after pulsed synthesis, the selectivity changes dramatically. P-Cu-1 displays 39.7% of C₂H₄ and 17.4% of CH₄ at −1.07 V vs RHE (Figure 4c). The formation of CH₄ on P-Cu-2 is further suppressed to 6.1% at −1.09 V vs RHE, whereas the FE of C₂H₄ is promoted to 48.6% (Figure 4d). Among these catalysts, the FE values of H₂ and CO are close with each other, and their major differences are attributed to the hydrocarbon selectivity. These results suggest that the preferred CO₂RR pathways on P-Cu catalysts are different compared with pristine polished Cu, and the former one should favor the C–C coupling to produce C₂ products. To understand the reason for different selectivities, the roughness factor (RF) was calculated by measuring double-layer capacitance (*C_{dl}*) after conducting the CO₂RR at various negative potentials according to the previously reported method (Figure S5, SI and Figure 4e).¹⁰ From polished Cu to P-Cu-2, the RF values increase, and this coincides with the increasing ratios of C₂H₄/CH₄, suggesting that an alternative oxidation and reduction process can deposit more Cu₂O on the surface and create a rougher porous film for efficient C₂H₄ production in CO₂RR. This is consistent with recent reports that have concluded the importance of surface roughness for C₂+ product production with Cu-based catalysts.^{43,44} Moreover, the catalytic activities of the 10 Cu foils synthesized in

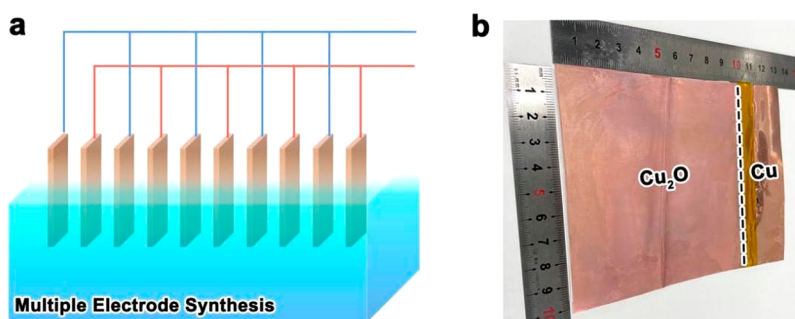


Figure 3. (a) Scaled setup for the synthesis of multiple electrodes. (b) Digital image of large-area electrode.

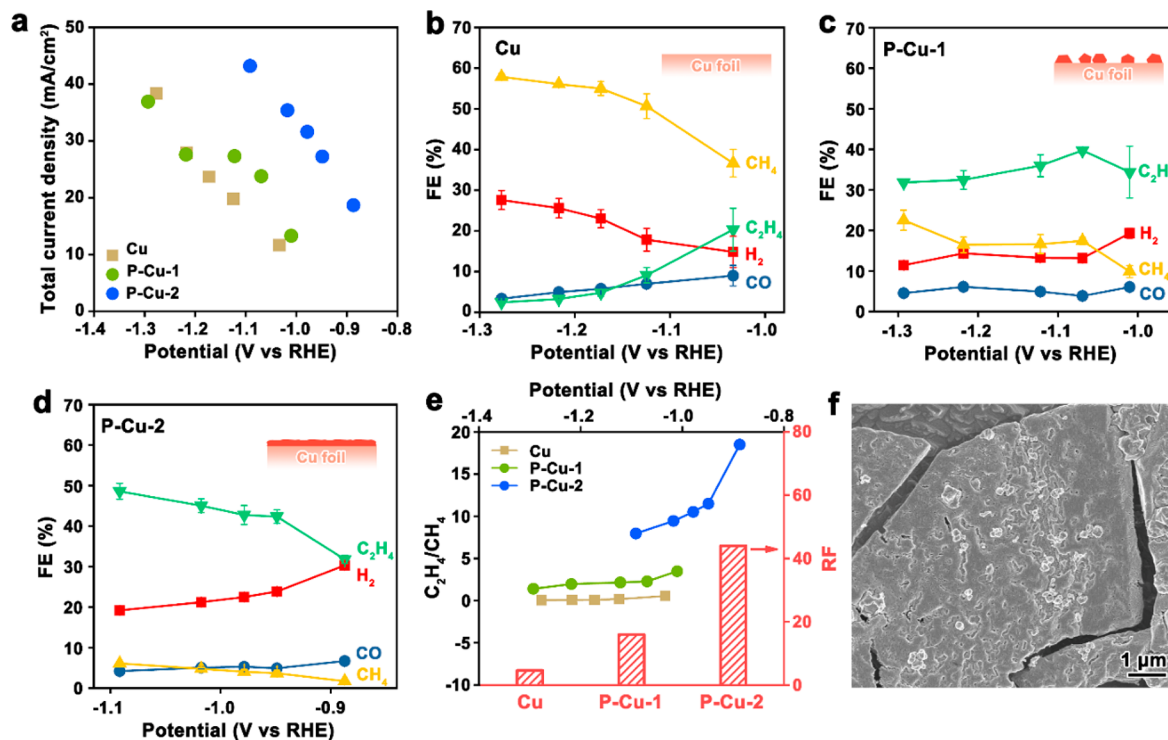


Figure 4. (a) Comparison of total geometric current density in CO₂RR catalyzed by polished Cu and P-Cu. FE of gaseous products on (b) polished Cu, (c) P-Cu-1, and (d) P-Cu-2. (e) Comparison of C₂H₄/CH₄ ratios and RF of different Cu-based catalysts. (f) SEM image of P-Cu after 2 h of CO₂RR electrolysis. An 85% iR correction was applied on the potentials in Figure 4.

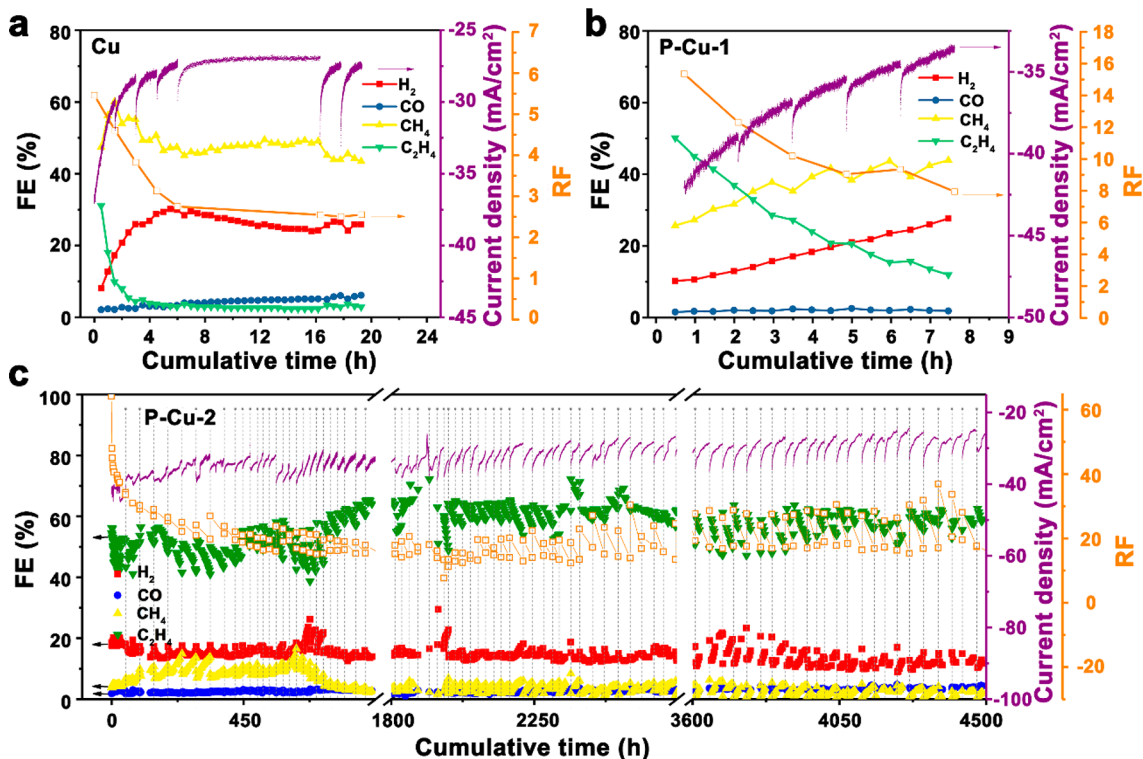


Figure 5. Stability evaluation for (a) polished Cu, (b) P-Cu-1, and (c) P-Cu-2; FE% of gaseous products is shown on the left y-axis, the corresponding current density is displayed on the right purple y-axis, the measured RF is plotted on the right orange y-axis, and the dashed vertical lines indicate the time when the electrolytes in both cathodic/anodic compartments are replaced.

one step are similar to each other in large part due to their similar structures after symmetric pulsed synthesis (Figure S6, SI). Besides the capability to synthesize multiple electrodes,

when using large-area Cu foil as the starting material, the CO₂RR catalyzed by six electrodes cut from enlarged Cu foil all demonstrate enhanced C₂H₄ FE (Figure S7, SI), showing

the good scalability of this method. Regarding the electrodes synthesized by constant potential deposition instead of the aforementioned pulsed deposition in a two-electrode system, the catalytic activities are slightly different (see [Supplementary Note 1](#) and [Figures S8–S10](#)). The presence of Cu^{2+} in the solution is important in order to achieve a catalytic film with high RF (see [Supplementary Note 2](#) and [Figure S11](#)).

Taken together, these results indicate that P-Cu catalysts are intrinsically more active to produce C_2^+ products during CO_2RR . CO is widely considered as the most important intermediate to produce C_2^+ products; the presence of a roughened surface, along with high porosity, can help to confine CO_2RR intermediates in the P-Cu catalysts, giving more time for the subsequent C–C coupling step and thus promoting C_2 products.^{11,12} A high RF also provides sufficient defective sites that bind with CO relatively strongly.⁴³ Therefore, the improved RF of the catalyst is responsible for the rapid rise of the C_2H_4 proportion. We also want to point out that P-Cu catalysts show significant structural and morphological changes after a few hours of CO_2RR ([Figure 4f](#) and [Supplementary Note 3](#); [Figures S12–S16](#) in SI). These observations prompt us to investigate more about the stability issue of these Cu-based catalysts in CO_2RR .

2.3. Evaluation of Long-Term Stability. Despite the significance, the stability is often less studied compared with other properties.^{23,26,45} Typically the lifetime for copper catalysts ranges from several hours to tens of hours, and only a few catalysts have been reported to operate for hundreds of hours to produce C_2^+ products.^{8,14,46,47} On the basis of the above discussion, RF is one of the important parameters that influences the catalytic activity and selectivity of copper-based catalysts in CO_2RR . Therefore, we monitored the RF of these catalysts during electrolysis by measuring C_{dl} to track possible changes of the catalyst to get more clues about structural evolutions of Cu during long-term CO_2RR . For the purpose of comparison, the long-term stability of polished Cu for CO_2RR was evaluated first, and the RF was monitored during CO_2RR ; as shown in [Figure 5a](#), the initial deactivation process is accompanied by a dramatic drop of RF. Both the current density and FE of C_2H_4 decline quickly in the initial few hours. The surface structure of polished Cu has minor changes after stability testing ([Figure S15](#), SI). The poor stability of polished Cu could be due to the formation of surface carbonaceous species.^{48,49} With regards to P-Cu-1, the stability and selectivity toward C_2H_4 is better than polished Cu, but the FE of C_2H_4 still drops below 20% after ~ 6 h of electrolysis, while CH_4 and H_2 become more dominant ([Figure 5b](#)). The reduced C_2H_4 FE is associated with the decreasing of RF, as verified by significant morphological changes of the catalyst after various times of CO_2RR electrolysis ([Figure S16a](#), SI). These results indicate that the loss of porosity/roughened surface strongly affects the activity and selectivity of CO_2RR .

To investigate more about the CO_2RR durability, the stability data of P-Cu-2 (i.e., synthesized after 900 pulsed cycles) was collected for a cumulative time of more than 6 months (ca. 4500 h), and C_2H_4 is still the primary product after such a long time ([Figure 5c](#) and [Figure S17](#), SI). To the best of our knowledge, this is the longest stability evaluation for Cu-based catalysts to produce C_2H_4 ([Table S1](#), SI). Surprisingly, the C_2H_4 FE is as high as 60%, and the CH_4 FE is below 5% even after 6 months of electrolysis. In general, after electrolysis in the same solution for some time, the ratio of $\text{C}_2\text{H}_4/\text{CH}_4$ would decrease, while the selectivity to C_2H_4 can

still recover in the fresh electrolyte ([Figure S18](#), SI). The change of selectivity is probably due to the increasing concentration of formate in the cathodic electrolyte.⁴⁸ Other C_2^+ liquid products, including ethanol, *n*-propanol, allyl alcohol, propionaldehyde, acetate, as well as some other organic compounds with small amounts, were identified in cathodic electrolyte after long-term electrolysis ([Figure S19](#), SI). The FE of major liquid products indicates that ethanol has the highest production rate with FE ranging from 6.4 to 14.7% among all the liquid products ([Figure S20](#), SI). It should be noted that some formate and acetate species were found in the anodic compartment, suggesting that these anions can transfer through an anion exchange membrane during long-term electrolysis. Considering both the gaseous and liquid products, the total FE for C_2^+ in CO_2RR is in the range of 70 to 80%.

The RF quickly drops from 64.5 to 37.6 during the first 30 h for P-Cu-2 and continues to trend down slowly thereafter ([Figure 5c](#)). After a few hundred hours of electrolysis, the RF values fluctuate between ~ 12 to 28, indicating that the structure of catalyst keeps changing continuously during long-term operation. Previous reports also confirm that the surface of Cu is very dynamic under the CO_2RR condition and can reconstruct based on *in situ/operando* observations.^{50,51} Our work proves that even with structural reconstruction, as long as the surface of Cu remains rough, represented by RF values, the P-Cu-2 electrode can catalyze CO_2RR with relatively stable C_2H_4 production for thousands of hours. For example, based on microscope observation, after ~ 1500 h of electrolysis, the surface of P-Cu-2 is still rough compared with polished Cu ([Figure S21](#), SI). When comparing the time-dependent RF trends of polished Cu and P-Cu ([Figure S22](#), SI), it is clear that the RF values decrease for all electrodes. However, only P-Cu-2 can keep relatively high RF values during stability testing. We believe that it is because isolated nanoparticles on P-Cu-1 are more vulnerable to degrade under the CO_2RR condition, while a robust catalytic film on P-Cu-2 is more stable during CO_2RR . In addition, even the RF of P-Cu-2 decreases obviously during the initial electrolysis, the value is significantly higher than the threshold value (~ 12 based on [Figure S22](#)), which helps to keep the C_2H_4 FE% stable. It should be noted that the catalytic film on P-Cu-2 is very robust, and no visible detachment of catalyst was found during long-term stability test ([Figure S23](#), SI). In terms of C_2H_4 production from CO_2RR , the previous longest stability evaluation in an H-cell is 240 h, and detachment of catalysts from the electrode was observed after stability evaluation.⁴⁷

To further understand the relationship of C_2H_4 selectivity and surface roughness, the FE of C_2H_4 and corresponding RF from polished Cu and P-Cu during stability measurement are summarized in one single graph ([Figure 6](#)). Clearly, we can draw a reliable conclusion that the C_2H_4 selectivity is strongly related with the RF of Cu catalysts. The C_2H_4 FE increases dramatically when the RF is in the small value range and thereafter reaches a maximum level. The formation of C_2 requires the confinement of C_1 intermediates in the pores as well as the existence of defective sites with stronger binding affinity with C_1 intermediates for further reduction; that is why a larger RF is beneficial for C_2H_4 formation. These results further prove that the selectivity of CO_2RR to hydrocarbons can be tuned by controlling the RF of Cu catalysts.

The current density in the H-cell is limited to tens of mA/cm^2 due to the low solubility of CO_2 in aqueous solution. In order to evaluate the stability of CO_2RR at high current

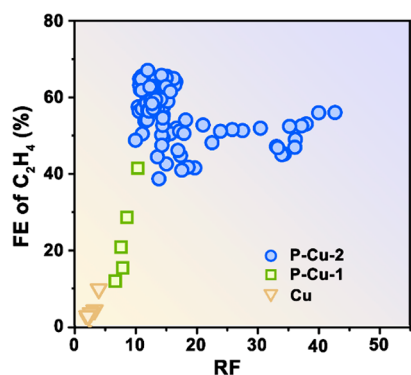


Figure 6. Relationship of C_2H_4 FE% and RF of copper-based catalysts.

density, pulsed copper on carbon paper was synthesized and used as a GDE in a flow cell (see [Supplementary Note 4](#)). At the current density of 200 mA/cm^2 , the FE of C_2H_4 can only maintain stable for a few hours because of the flooding issue ([Figure S24](#)). It should be noted that the stability of CO_2RR in flow cell is at least related with three factors: first is the catalyst stability, second is the ability to maintain a gas/liquid/solid triple phase and avoid the flooding problem, and third is the formation of carbonate salts, which can block the transport pathways in the gas diffusion layer.²⁷ On the contrary, the stability is mainly determined by the catalyst itself in H-cell. Our work proves that as long as the copper surface remains rough, it can deliver a stable C_2H_4 FE% in CO_2RR in the H-cell. However, we do believe that there is a lot more work required in the future to solve other problems that fail the GDE.

3. CONCLUSION

In summary, we have developed a facile pulsed potential method to synthesize Cu_2O catalysts for CO_2RR with stable C_2H_4 production for over 4500 h. By using this method, two active electrodes can be synthesized at the same time, and the number of synthesized electrodes could be boosted even higher by using a scaled setup. The clear result of this study shows that a larger RF promotes the reaction pathway of CO_2RR toward ethylene production. These findings provide important insights on the activity and selectivity changes during long-term CO_2RR .

4. EXPERIMENTAL SECTION

4.1. Chemicals and Reagents. Copper foil (0.3 mm thickness, 13 mm wideness, 99.9% metals basis), copper with a bigger size (AR, 99.5% metals basis), phosphoric acid (85 wt % in water, 99.99% metals basis), $KHCO_3$ (99.99% metals basis), and dimethyl sulfoxide were purchased from Shanghai Macklin Biochemical Co., Ltd. $CuSO_4 \cdot 5H_2O$ (99.99% metals basis) was purchased from Shanghai Aladdin Biochemical Co., Ltd. The Cu foils were electrochemically polished by applying a voltage of +4 V versus a titanium plate for 5 min. Ultrapure water ($18.2 \text{ M}\Omega \cdot \text{cm}$), purified by Aquaplore, was used in all the experiments.

4.2. Pulsed Potential Synthesis. A two-electrode electrochemical cell was constructed by placing two electrochemically polished Cu foils in parallel in 0.1 M $CuSO_4$ solution (ca. 1 cm^2 of Cu was exposed to the electrolyte). The potential values between two Cu foils were controlled by a CH Instrument 440C potentiostat as follows: +2.0 V for 1 s and −2.0 V for 1 s. The above pulsed potential program was repeated for 10 and 900 cycles. After a one-step

electrosynthesis, both of the Cu electrodes were carefully cleaned with ultrapure water and dried under an ambient condition.

4.3. Electrode Characterizations. The surface of the electrode was observed by a ZEISS Sigma 300 scanning electron microscope (SEM). The optical microscope images were taken by Olympus (Nikon). X-ray photoelectron spectroscopy (XPS) was performed using a Thermo Scientific K-Alpha Nexsa (Al $K\alpha$ emission source). The spectra of copper $2p_{3/2}$ were aligned to 932.67 eV, corresponding to the binding energy of Cu/Cu_2O .⁵² Grazing incident X-ray diffraction (GIXRD) of the electrode was recorded with a Rigaku SmartLab in the range of $20\text{--}80^\circ$ at a step scanning rate of $2^\circ/\text{min}$ (Cu $K\alpha$, 40 kV, 30 mA). The incoming X-ray angle was kept at 0.1° . Raman spectroscopy was carried out on a Horiba HR Evolution with a 532 nm laser source.

4.4. CO_2 Reduction Evaluation. The electrochemical measurements were performed on a CH Instruments 760E potentiostat. $KHCO_3$ solution (0.1 M) saturated with CO_2 was used as electrolyte for CO_2 reduction evaluation. The as-synthesized Cu electrodes were directly used as the WE. A piece of platinum foil was used as the CE. $Ag/AgCl$ electrode filled with 3.0 M KCl solution served as the RE.

Electrolysis was conducted in a gas-tight H-cell separated by a piece of Selenion anion exchange membrane (AMV, $120 \mu\text{m}$). Anodic and cathodic compartments all contained 60 mL of 0.1 M $KHCO_3$ electrolyte. The solution in the cathodic side was purged with CO_2 (99.999%) for 20 min to allow the saturation of electrolyte with CO_2 before the experiment. During the bulk electrolysis, CO_2 was bubbled through the cathodic electrolyte at a constant rate of 10.000 sccm controlled by a digital mass flow controller (Cole-Parmer). The solution was continuously stirred at 400 rpm. The unreacted CO_2 as well as the gaseous products were directly vented into the gas chromatograph (Agilent 7890B) to quantify the products. The GC was equipped with a combination of a MolSieve 5 A column (8 ft, 1/8 in., 2 mm), a HayeSep Q column (3 ft, 1/8 in., 2 mm), a HayeSep Q column (6 ft, 1/8 in., 2 mm), and an HP-PLOT/Q column (0.32 mm). A thermal conductivity detector (TCD) was used to determine H_2 concentration, hydrocarbon products such as CH_4 and C_2H_4 were quantified by a flame ionization detector (FID), and CO was detected by an FID with methanizer. A certified standard gas mixture consisting of 0.507% H_2 , 0.102% CO, 0.503% CH_4 , 0.3% C_2H_4 , 0.0099% C_2H_6 , and 0.01% C_3H_6 (propylene) balanced with CO_2 was purchased from Dalian Special Gases Co., Ltd. to calibrate the GC. The FE was calculated based on the following equation

$$FE_{\text{gas}} = (x_i \times V_j \times v \times F \times P) / (R \times T \times i) \quad (1)$$

where x_i is the number of electrons required to form a specific reduction product, V_j (vol %) is the volume concentration of the product in the gas phase ($J = CO, CH_4, C_2H_4$, or H_2), v (m^3/s) is the gas flow rate controlled by the digital mass flow controller, i (A) is the steady-state cell current, and other parameters are listed here: $P = 1.01 \times 10^5 \text{ Pa}$, $T = 298.15 \text{ K}$, $F = 96485 \text{ C/mol}$, and $R = 8.314 \text{ Jmol}^{-1} \text{ K}^{-1}$.

Liquid products were analyzed on a JEOL 400 MHz NMR spectrometer. A 0.3 mL aliquot of the electrolyte was mixed with 0.3 mL of D_2O , and dimethyl sulfoxide (DMSO) was added as an internal standard. The water suppression method was used for the measurement. The FE of liquid products was calculated according to the following equation

$$FE_{\text{liquid}} = (n \times x_i \times F) / Q \quad (2)$$

where n is the number of moles of product, x_i is the number of electrons required to form liquid products, F (96 485 C/mol) is the Faraday constant, and Q (C) is the quantity of electric charge during constant electrolysis.

For multiple potential electrolysis, all the potential values measured against the RE were converted to the RHE using the following equation

$$E(\text{vs. RHE}) = E(\text{vs. Ag/AgCl}) + 0.210 \text{ V} + 0.0592 \text{ V} \times \text{pH} \quad (3)$$

An 85% *iR* compensation was performed. The system resistance R_s was calculated according to electrochemical impedance data. For the stability test, the constant potential electrolysis was performed at -2.2 V vs Ag/AgCl, and this value is not *iR*-corrected because of the fluctuation of current during the stability test.

4.5. Double-Layer Capacitance and Roughness Factor Determination. The double-layer capacitance (C_{dl}) was measured by recording the CV curves at a series of scan rates (0.08, 0.06, 0.04, 0.02, 0.01, and 0.005 V/s) in a non-Faradaic potential window from -0.76 to -0.66 V vs Ag/AgCl in 0.1 M KHCO_3 . Half of the differences of the anodic and cathodic current values (mA) at -0.71 V vs Ag/AgCl were plotted against the scan rates (V/s) and fitted linearly to calculate the slope, which equals the capacitance of the electrode.

The C_{dl} normalized by the geometric area of the electrode was calculated based on the following equation

$$C_{dl} = S/A \quad (4)$$

where A represents the geometric area of the electrode and S equals the slope of the fitted line. To calculate RF of the electrodes, the specific capacitance of flat polycrystalline copper foil ($C_{ref} = 0.029$ mF/cm², RF = 1) is obtained from previous reports, and the following equation is used^{10,18}

$$RF = C_{dl}/C_{ref} \quad (5)$$

■ ASSOCIATED CONTENT

SI Supporting Information

The Supporting Information is available free of charge at <https://pubs.acs.org/doi/10.1021/acsami.2c01230>.

Current versus time curves during electrode synthesis, GIXRD and SEM images of as-synthesized pulsed Cu-based catalysts, photograph of the setup to synthesize 10 P-Cu at the same time, double-layer capacitance measurement, CO₂RR performance of multiple electrodes synthesized in one step, CO₂RR performance of a large-area electrode, discussion about influence of the deposition method on catalytic selectivity, discussion about the influence of the electrolyte on catalytic performance, characterization of P-Cu after short-term CO₂RR, long-term stability evaluation of CO₂RR, and the evaluation in flow cell (PDF)

■ AUTHOR INFORMATION

Corresponding Authors

Xiaoxi Huang – Hoffmann Institute of Advanced Materials, Postdoctoral Innovation Practice Base, Shenzhen Polytechnic, Shenzhen 518055, P. R. China; orcid.org/0000-0002-1975-2312; Email: xiaoxihuang@szpt.edu.cn

Xiaoxin Zou – State Key Laboratory of Inorganic Synthesis and Preparative Chemistry, College of Chemistry, Jilin University, 130012 Changchun, P. R. China; orcid.org/0000-0003-4143-9274; Email: xxzou@jlu.edu.cn

Authors

Jian Zhang – Hoffmann Institute of Advanced Materials, Postdoctoral Innovation Practice Base, Shenzhen Polytechnic, Shenzhen 518055, P. R. China; School of Chemistry and Chemical Engineering, South China University of Technology, Guangzhou 510640, P. R. China

Zhipeng Liu – Hoffmann Institute of Advanced Materials, Postdoctoral Innovation Practice Base, Shenzhen Polytechnic, Shenzhen 518055, P. R. China; Shenzhen Institutes of Advanced Technology, Chinese Academy of Sciences, Shenzhen 518055, P. R. China

Hongshan Guo – Hoffmann Institute of Advanced Materials, Postdoctoral Innovation Practice Base, Shenzhen Polytechnic, Shenzhen 518055, P. R. China

Haoran Lin – Hoffmann Institute of Advanced Materials, Postdoctoral Innovation Practice Base, Shenzhen Polytechnic, Shenzhen 518055, P. R. China; orcid.org/0000-0003-0625-8881

Hao Wang – Hoffmann Institute of Advanced Materials, Postdoctoral Innovation Practice Base, Shenzhen Polytechnic, Shenzhen 518055, P. R. China; orcid.org/0000-0001-7732-778X

Xiao Liang – State Key Laboratory of Inorganic Synthesis and Preparative Chemistry, College of Chemistry, Jilin University, 130012 Changchun, P. R. China

Hanlin Hu – Hoffmann Institute of Advanced Materials, Postdoctoral Innovation Practice Base, Shenzhen Polytechnic, Shenzhen 518055, P. R. China; orcid.org/0000-0001-5617-0998

Qibin Xia – School of Chemistry and Chemical Engineering, South China University of Technology, Guangzhou 510640, P. R. China; orcid.org/0000-0002-8563-6715

Complete contact information is available at:

<https://pubs.acs.org/doi/10.1021/acsami.2c01230>

Author Contributions

X.H. conceived the idea, analyzed the results, and supervised the project, J.Z. carried out catalyst synthesis and characterizations as well as the evaluation of CO₂RR performance, Z.L. analyzed the data and designed the graphs, H.G. assisted with the electrochemical measurement, H.L. helped with NMR measurement, H.W. assisted with GC measurement, X.L. designed and drew the graphs, H.H. assisted with the electrode synthesis, X.Z. assisted with experimental design, X.H. and X.Z. wrote the manuscript with input from all authors. J.Z. and Q.X. assisted with the revision of manuscript. All authors discussed the results and helped with the manuscript preparation. All authors have given approval to the final version of the manuscript.

Notes

The authors declare no competing financial interest.

■ ACKNOWLEDGMENTS

This work is supported by the Scientific and Technical Innovation Council of Shenzhen (Task Book No. GXWD20201231165806004, Project No. 20200828014156001) and Shenzhen Polytechnic.

■ REFERENCES

- (1) De Luna, P.; Hahn, C.; Higgins, D.; Jaffer, S. A.; Jaramillo, T. F.; Sargent, E. H. What Would it Take for Renewably Powered Electrosynthesis to Displace Petrochemical Processes? *Science* **2019**, 364, No. eaav3506.
- (2) Nitopi, S.; Bertheussen, E.; Scott, S. B.; Liu, X.; Engstfeld, A. K.; Horch, S.; Seger, B.; Stephens, I. E. L.; Chan, K.; Hahn, C.; Nørskov, J. K.; Jaramillo, T. F.; Chorkendorff, I. Progress and Perspectives of Electrochemical CO₂ Reduction on Copper in Aqueous Electrolyte. *Chem. Rev.* **2019**, 119, 7610–7672.
- (3) Gattrell, M.; Gupta, N.; Co, A. A Review of the Aqueous Electrochemical Reduction of CO₂ to Hydrocarbons at Copper. *J. Electroanal. Chem.* **2006**, 594, 1–19.
- (4) Kuhl, K. P.; Cave, E. R.; Abram, D. N.; Jaramillo, T. F. New Insights into the Electrochemical Reduction of Carbon Dioxide on Metallic Copper Surfaces. *Energy Environ. Sci.* **2012**, 5, 7050–7059.

- (5) Xu, S.; Carter, E. A. Theoretical Insights into Heterogeneous (Photo)electrochemical CO₂ Reduction. *Chem. Rev.* **2019**, *119*, 6631–6669.
- (6) Peterson, A. A.; Abild-Pedersen, F.; Studt, F.; Rossmeisl, J.; Nørskov, J. K. How Copper Catalyzes the Electroreduction of Carbon Dioxide into Hydrocarbon Fuels. *Energy Environ. Sci.* **2010**, *3*, 1311–1315.
- (7) Perez-Gallent, E.; Figueiredo, M. C.; Calle-Vallejo, F.; Koper, M. T. Spectroscopic Observation of a Hydrogenated CO Dimer Intermediate During CO Reduction on Cu(100) Electrodes. *Angew. Chem., Int. Ed.* **2017**, *56*, 3621–3624.
- (8) Li, F.; Thevenon, A.; Rosas-Hernandez, A.; Wang, Z.; Li, Y.; Gabardo, C. M.; Ozden, A.; Dinh, C. T.; Li, J.; Wang, Y.; Edwards, J. P.; Xu, Y.; McCallum, C.; Tao, L.; Liang, Z. Q.; Luo, M.; Wang, X.; Li, H.; O'Brien, C. P.; Tan, C. S.; Nam, D. H.; Quintero-Bermudez, R.; Zhuang, T. T.; Li, Y. C.; Han, Z.; Britt, R. D.; Sinton, D.; Agapie, T.; Peters, J. C.; Sargent, E. H. Molecular Tuning of CO₂-to-Ethylene Conversion. *Nature* **2020**, *577*, 509–513.
- (9) Chen, X.; Chen, J.; Alghoraibi, N. M.; Henckel, D. A.; Zhang, R.; Nwabara, U. O.; Madsen, K. E.; Kenis, P. J. A.; Zimmerman, S. C.; Gewirth, A. A. Electrochemical CO₂-to-Ethylene Conversion on Polyamine-Incorporated Cu Electrodes. *Nat. Catal.* **2021**, *4*, 20–27.
- (10) Wang, L.; Nitopi, S.; Wong, A. B.; Snider, J. L.; Nielander, A. C.; Morales-Guio, C. G.; Orazov, M.; Higgins, D. C.; Hahn, C.; Jaramillo, T. F. Electrochemically Converting Carbon Monoxide to Liquid Fuels by Directing Selectivity with Electrode Surface Area. *Nat. Catal.* **2019**, *2*, 702–708.
- (11) Zhuang, T.-T.; Pang, Y.; Liang, Z.-Q.; Wang, Z.; Li, Y.; Tan, C.-S.; Li, J.; Dinh, C. T.; De Luna, P.; Hsieh, P.-L.; Burdyny, T.; Li, H.-H.; Liu, M.; Wang, Y.; Li, F.; Proppe, A.; Johnston, A.; Nam, D.-H.; Wu, Z.-Y.; Zheng, Y.-R.; Ip, A. H.; Tan, H.; Chen, L.-J.; Yu, S.-H.; Kelley, S. O.; Sinton, D.; Sargent, E. H. Copper Nanocavities Confine Intermediates for Efficient Electrosynthesis of C₃ Alcohol Fuels from Carbon Monoxide. *Nat. Catal.* **2018**, *1*, 946–951.
- (12) Yang, P. P.; Zhang, X. L.; Gao, F. Y.; Zheng, Y. R.; Niu, Z. Z.; Yu, X.; Liu, R.; Wu, Z. Z.; Qin, S.; Chi, L. P.; Duan, Y.; Ma, T.; Zheng, X. S.; Zhu, J.; Wang, H. J.; Gao, M. R.; Yu, S. H. Protecting Copper Oxidation State via Intermediate Confinement for Selective CO₂ Electroreduction to C₂⁺ Fuels. *J. Am. Chem. Soc.* **2020**, *142*, 6400–6408.
- (13) Jiang, K.; Sandberg, R. B.; Akey, A. J.; Liu, X.; Bell, D. C.; Nørskov, J. K.; Chan, K.; Wang, H. Metal Ion Cycling of Cu Foil for Selective C–C Coupling in Electrochemical CO₂ Reduction. *Nat. Catal.* **2018**, *1*, 111–119.
- (14) Choi, C.; Kwon, S.; Cheng, T.; Xu, M.; Tieu, P.; Lee, C.; Cai, J.; Lee, H. M.; Pan, X.; Duan, X.; Goddard, W. A.; Huang, Y. Highly Active and Stable Stepped Cu Surface for Enhanced Electrochemical CO₂ Reduction to C₂H₄. *Nat. Catal.* **2020**, *3*, 804–812.
- (15) Wang, Y.; Wang, Z.; Dinh, C.-T.; Li, J.; Ozden, A.; Golam Kibria, M.; Seifitokaldani, A.; Tan, C.-S.; Gabardo, C. M.; Luo, M.; Zhou, H.; Li, F.; Lum, Y.; McCallum, C.; Xu, Y.; Liu, M.; Proppe, A.; Johnston, A.; Todorovic, P.; Zhuang, T.-T.; Sinton, D.; Kelley, S. O.; Sargent, E. H. Catalyst Synthesis under CO₂ Electroreduction Favours Faceting and Promotes Renewable Fuels Electrosynthesis. *Nat. Catal.* **2020**, *3*, 98–106.
- (16) Suen, N.-T.; Kong, Z.-R.; Hsu, C.-S.; Chen, H.-C.; Tung, C.-W.; Lu, Y.-R.; Dong, C.-L.; Shen, C.-C.; Chung, J.-C.; Chen, H. M. Morphology Manipulation of Copper Nanocrystals and Product Selectivity in the Electrocatalytic Reduction of Carbon Dioxide. *ACS Catal.* **2019**, *9*, S217–S222.
- (17) Cheng, D.; Zhao, Z. J.; Zhang, G.; Yang, P.; Li, L.; Gao, H.; Liu, S.; Chang, X.; Chen, S.; Wang, T.; Ozin, G. A.; Liu, Z.; Gong, J. The Nature of Active Sites for Carbon Dioxide Electroreduction over Oxide-Derived Copper Catalysts. *Nat. Commun.* **2021**, *12*, 395.
- (18) Li, C. W.; Kanan, M. W. CO₂ Reduction at Low Overpotential on Cu Electrodes Resulting from the Reduction of Thick Cu₂O Films. *J. Am. Chem. Soc.* **2012**, *134*, 7231–7234.
- (19) Li, C. W.; Ciston, J.; Kanan, M. W. Electroreduction of Carbon Monoxide to Liquid Fuel on Oxide-Derived Nanocrystalline Copper. *Nature* **2014**, *508*, 504–507.
- (20) Grosse, P.; Gao, D.; Scholten, F.; Sinev, I.; Mistry, H.; Roldan Cuenya, B. Dynamic Changes in the Structure, Chemical State and Catalytic Selectivity of Cu Nanocubes during CO₂ Electroreduction: Size and Support Effects. *Angew. Chem., Int. Ed.* **2018**, *57*, 6192–6197.
- (21) Li, Y.; Kim, D.; Louisia, S.; Xie, C.; Kong, Q.; Yu, S.; Lin, T.; Aloni, S.; Fakra, S. C.; Yang, P. Electrochemically Scrambled Nanocrystals are Catalytically Active for CO₂-to-Multicarbon. *Proc. Natl. Acad. Sci. U.S.A.* **2020**, *117*, 9194–9201.
- (22) Huang, J.; Hormann, N.; Oveisi, E.; Loiudice, A.; De Gregorio, G. L.; Andreussi, O.; Marzari, N.; Buonsanti, R. Potential-Induced Nanoclustering of Metallic Catalysts during Electrochemical CO₂ Reduction. *Nat. Commun.* **2018**, *9*, 3117.
- (23) Popovic, S.; Smiljanic, M.; Jovanovic, P.; Vavra, J.; Buonsanti, R.; Hodnik, N. Stability and Degradation Mechanisms of Copper-Based Catalysts for Electrochemical CO₂ Reduction. *Angew. Chem., Int. Ed.* **2020**, *59*, 14736–14746.
- (24) Kutz, R. B.; Chen, Q.; Yang, H.; Sajjad, S. D.; Liu, Z.; Masel, I. R. Sustainion Imidazolium-Functionalized Polymers for Carbon Dioxide Electrolysis. *Energy Technol.* **2017**, *5*, 929–936.
- (25) Haas, T.; Krause, R.; Weber, R.; Demler, M.; Schmid, G. Technical Photosynthesis Involving CO₂ Electrolysis and Fermentation. *Nat. Catal.* **2018**, *1*, 32–39.
- (26) Nwabara, U. O.; Cofell, E. R.; Verma, S.; Negro, E.; Kenis, P. J. A. Durable Cathodes and Electrolyzers for the Efficient Aqueous Electrochemical Reduction of CO₂. *ChemSusChem* **2020**, *13*, 855–875.
- (27) Wakerley, D.; Lamaison, S.; Wicks, J.; Clemens, A.; Feaster, J.; Corral, D.; Jaffer, S. A.; Sarkar, A.; Fontcave, M.; Duoss, E. B.; Baker, S.; Sargent, E. H.; Jaramillo, T. F.; Hahn, C. Gas Diffusion Electrodes, Reactor Designs and Key Metrics of Low-Temperature CO₂ Electrolysers. *Nat. Energy* **2022**, *7*, 130–143.
- (28) Kim, D.; Lee, S.; Ocon, J. D.; Jeong, B.; Lee, J. K.; Lee, J. Insights into an Autonomously formed Oxygen-Evacuated Cu₂O Electrode for the Selective Production of C₂H₄ from CO₂. *Phys. Chem. Chem. Phys.* **2015**, *17*, 824–830.
- (29) Lee, S. Y.; Jung, H.; Kim, N. K.; Oh, H. S.; Min, B. K.; Hwang, Y. J. Mixed Copper States in Anodized Cu Electrocatalyst for Stable and Selective Ethylene Production from CO₂ Reduction. *J. Am. Chem. Soc.* **2018**, *140*, 8681–8689.
- (30) Verdager-Casadevall, A.; Li, C. W.; Johansson, T. P.; Scott, S. B.; McKeown, J. T.; Kumar, M.; Stephens, I. E.; Kanan, M. W.; Chorkendorff, I. Probing the Active Surface Sites for CO Reduction on Oxide-Derived Copper Electrocatalysts. *J. Am. Chem. Soc.* **2015**, *137*, 9808–9811.
- (31) Feng, X.; Jiang, K.; Fan, S.; Kanan, M. W. A Direct Grain-Boundary-Activity Correlation for CO Electroreduction on Cu Nanoparticles. *ACS Cent. Sci.* **2016**, *2*, 169–174.
- (32) Mariano, R. G.; McKelvey, K.; White, H. S.; Kanan, M. W. Selective Increase in CO₂ Electroreduction Activity at Grain-Boundary Surface Terminations. *Science* **2017**, *358*, 1187–1192.
- (33) Handoko, A. D.; Chan, K. W.; Yeo, B. S. -CH₃Mediated Pathway for the Electroreduction of CO₂ to Ethane and Ethanol on Thick Oxide-Derived Copper Catalysts at Low Overpotentials. *ACS Energy Lett.* **2017**, *2*, 2103–2109.
- (34) Ren, D.; Deng, Y.; Handoko, A. D.; Chen, C. S.; Malkhandi, S.; Yeo, B. S. Selective Electrochemical Reduction of Carbon Dioxide to Ethylene and Ethanol on Copper(I) Oxide Catalysts. *ACS Catal.* **2015**, *5*, 2814–2821.
- (35) Kas, R.; Kortlever, R.; Milbrat, A.; Koper, M. T.; Mul, G.; Baltrusaitis, J. Electrochemical CO₂ Reduction on Cu₂O-Derived Copper Nanoparticles: Controlling the Catalytic Selectivity of Hydrocarbons. *Phys. Chem. Chem. Phys.* **2014**, *16*, 12194–12201.
- (36) Lum, Y.; Ager, J. W. Stability of Residual Oxides in Oxide-Derived Copper Catalysts for Electrochemical CO₂ Reduction Investigated with (18) O Labeling. *Angew. Chem., Int. Ed.* **2018**, *57*, 551–554.

- (37) Li, J.; Kuang, Y.; Meng, Y.; Tian, X.; Hung, W. H.; Zhang, X.; Li, A.; Xu, M.; Zhou, W.; Ku, C. S.; Chiang, C. Y.; Zhu, G.; Guo, J.; Sun, X.; Dai, H. Electrodreduction of CO₂ to Formate on a Copper-Based Electrocatalyst at High Pressures with High Energy Conversion Efficiency. *J. Am. Chem. Soc.* **2020**, *142*, 7276–7282.
- (38) Ma, M.; Djanashvili, K.; Smith, W. A. Controllable Hydrocarbon Formation from the Electrochemical Reduction of CO₂ over Cu Nanowire Arrays. *Angew. Chem., Int. Ed.* **2016**, *55*, 6680–4.
- (39) Zhang, W.; Huang, C.; Xiao, Q.; Yu, L.; Shuai, L.; An, P.; Zhang, J.; Qiu, M.; Ren, Z.; Yu, Y. Atypical Oxygen-bearing Copper Boosts Ethylene Selectivity toward Electrocatalytic CO₂ Reduction. *J. Am. Chem. Soc.* **2020**, *142*, 11417–11427.
- (40) Mistry, H.; Varela, A. S.; Bonifacio, C. S.; Zegkinoglou, I.; Sinev, I.; Choi, Y. W.; Kisslinger, K.; Stach, E. A.; Yang, J. C.; Strasser, P.; Cuenya, B. R. Highly Selective Plasma-Activated Copper Catalysts for Carbon Dioxide Reduction to Ethylene. *Nat. Commun.* **2016**, *7*, 12123.
- (41) Rahaman, M.; Dutta, A.; Zanetti, A.; Broekmann, P. Electrochemical Reduction of CO₂ into Multicarbon Alcohols on Activated Cu Mesh Catalysts: An Identical Location (IL) Study. *ACS Catal.* **2017**, *7*, 7946–7956.
- (42) Zhao, K.; Liu, Y.; Quan, X.; Chen, S.; Yu, H. CO₂ Electrodreduction at Low Overpotential on Oxide-Derived Cu/Carbons Fabricated from Metal Organic Framework. *ACS Appl. Mater. Interfaces* **2017**, *9*, 5302–5311.
- (43) Jiang, K.; Huang, Y.; Zeng, G.; Toma, F. M.; Goddard, W. A.; Bell, A. T. Effects of Surface Roughness on the Electrochemical Reduction of CO₂ over Cu. *ACS Energy Lett.* **2020**, *5*, 1206–1214.
- (44) Gauthier, J. A.; Stenlid, J. H.; Abild-Pedersen, F.; Head-Gordon, M.; Bell, A. T. The Role of Roughening to Enhance Selectivity to C₂+ Products during CO₂ Electrodreduction on Copper. *ACS Energy Letters* **2021**, *6*, 3252–3260.
- (45) Choi, W.; Won, D. H.; Hwang, Y. J. Catalyst Design Strategies for Stable Electrochemical CO₂ Reduction Reaction. *J. Mater. Chem. A* **2020**, *8*, 15341–15357.
- (46) Dinh, C.-T.; Burdyny, T.; Kibria, M. G.; Seifitokaldani, A.; Gabardo, C. M.; García de Arquer, F. P.; Kiani, A.; Edwards, J. P.; De Luna, P.; Bushuyev, O. S.; Zou, C.; Quintero-Bermudez, R.; Pang, Y.; Sinton, D.; Sargent, E. H. CO₂ Electrodreduction to Ethylene via Hydroxide-Mediated Copper Catalysis at an Abrupt Interface. *Science* **2018**, *360*, 783–787.
- (47) Yang, J.; Li, M.; Ma, Y.; Chen, J.; Luo, W.; Sacchi, M.; Jiang, W.; Lawrence, R. Residual Chlorine Induced Cationic Active Species on Porous Cu Electrocatalyst for Highly Stable Electrochemical CO₂ Reduction to C₂. *Angew. Chem., Int. Ed.* **2021**, *60*, 11487–11493.
- (48) DeWulf, D. W.; Jin, T.; Bard, A. J. Electrochemical and Surface Studies of Carbon Dioxide Reduction to Methane and Ethylene at Copper Electrodes in Aqueous Solutions. *J. Electrochem. Soc.* **1989**, *136*, 1686–1691.
- (49) Weng, Z.; Zhang, X.; Wu, Y.; Huo, S.; Jiang, J.; Liu, W.; He, G.; Liang, Y.; Wang, H. Self-Cleaning Catalyst Electrodes for Stabilized CO₂ Reduction to Hydrocarbons. *Angew. Chem., Int. Ed.* **2017**, *56*, 13135–13139.
- (50) Vavra, J.; Shen, T. H.; Stoian, D.; Tileli, V.; Buonsanti, R. Real-time Monitoring Reveals Dissolution/Redeposition Mechanism in Copper Nanocatalysts during the Initial Stages of the CO₂ Reduction Reaction. *Angew. Chem., Int. Ed.* **2021**, *60*, 1347–1354.
- (51) Popovic, S.; Bele, M.; Hodnik, N. Reconstruction of Copper Nanoparticles at Electrochemical CO₂ Reduction Reaction Conditions Occurs via Two-step Dissolution/Redeposition Mechanism. *ChemElectroChem* **2021**, *8*, 2634–2639.
- (52) Arán-Ais, R. M.; Scholten, F.; Kunze, S.; Rizo, R.; Roldan Cuenya, B. The Role of in situ Generated Morphological Motifs and Cu(i) Species in C₂+ Product Selectivity during CO₂ Pulsed Electrodreduction. *Nat. Energy* **2020**, *5*, 317–325.